Aalborg Universitet

Small-Scale Testing of Laterally Loaded Non-Slender Monopiles in Sand

Thomassen, Kristina; Roesen, Hanne Ravn; Ibsen, Lars Bo; Sørensen, Søren Peder Hyldal

Link to publication from Aalborg University

Small-Scale Testing of Laterally Loaded Non-Slender Monopiles in Sand

K. Thomassen
H. R. Roesen
L. B. Ibsen
S. P. H. Sørensen

AALBORG UNIVERSITY

Department of Civil Engineering

Aalborg University
Department of Civil Engineering
Division of Water and Soil

Small-Scale Testing of Laterally Loaded Non-Slender Monopiles in Sand

by

K. Thomassen
H. R. Roesen
L. B. Ibsen
S. P. H. Sørensen

June 2010

Scientific Publications at the Department of Civil Engineering

Technical Reports are published for timely dissemination of research results and scientific work carried out at the Department of Civil Engineering (DCE) at Aalborg University. This medium allows publication of more detailed explanations and results than typically allowed in scientific journals.

Technical Memoranda are produced to enable the preliminary dissemination of scientific work by the personnel of the DCE where such release is deemed to be appropriate. Documents of this kind may be incomplete or temporary versions of papers—or part of continuing work. This should be kept in mind when references are given to publications of this kind.

Contract Reports are produced to report scientific work carried out under contract. Publications of this kind contain confidential matter and are reserved for the sponsors and the DCE. Therefore, Contract Reports are generally not available for public circulation.

Lecture Notes contain material produced by the lecturers at the DCE for educational purposes. This may be scientific notes, lecture books, example problems or manuals for laboratory work, or computer programs developed at the DCE.

Theses are monograms or collections of papers published to report the scientific work carried out at the DCE to obtain a degree as either PhD or Doctor of Technology. The thesis is publicly available after the defence of the degree.

Latest News is published to enable rapid communication of information about scientific work carried out at the DCE. This includes the status of research projects, developments in the laboratories, information about collaborative work and recent research results.

Small-Scale Testing of Laterally Loaded Non-Slender Monopiles in Sand

K. Thomassen[1]; H. R. Roesen[1]; L. B. Ibsen[2]; and S. P. H. Sørensen[3]

Aalborg University, June 2010

Abstract

In current design of offshore wind turbines, monopiles are often used as foundation. The behaviour of the monopiles when subjected to lateral loading has not been fully investigated, e.g. the diameter effect on the soil response. In this paper the behaviour of two non-slender aluminium piles in sand subjected to lateral loading are analysed by means of small-scale laboratory tests. The six quasi-static tests are conducted on piles with diameters of 40 mm and 100 mm and a slenderness ratio, L/D, of 5. In order to minimise scale effects, the tests are carried out in a pressure tank at stress levels of 0 kPa, 50 kPa, and 100 kPa, respectively. From the tests load-deflection relationships of the piles at three levels above the soil surface are obtained. The load-deflection relationships reveal that the uncertainties of the results for the pile with diameter of 40 mm are large due to the small soil volume activated during failure. From the load-deflection relationships normalised as $H/(L^2 D \gamma')$ and y/D indicates that the lateral load, H, is proportional to the embedded length square times the pile diameter, $L^2 D$. Furthermore, by comparing the normalised load-deflection relationships for different stress levels it is seen that small-scale tests with overburden pressure applied is preferable.

1 Introduction

In the design of laterally loaded monopiles the $p-y$ curve method given in the design regulations API (1993) and DNV (1992) is often used. For piles in sand the recommended $p-y$ curves are based on results from two slender, flexible piles with a slenderness ratio $L/D = 34.4$ where L is the embedded length and D is the diameter. Contrary to the assumption of flexible piles for these curves the monopile foundations installed today has a slenderness ratio $L/D < 10$, and behaves almost as rigid objects. The recommended curves does not take the effect of the slenderness ratio into account. Furthermore, the initial stiffness is considered independent of the pile properties such as the pile diameter. The research within the field of diameter effects gives contradictory conclusions. Different studies have shown the initial stiffness to be either independent, linearly dependent, or non-linear dependent on the pile diameter, cf. Brødbæk et al. (2009).

This paper evaluates the effects of the pile diameter on the soil resistance through six small-scale tests.

---

[1]Graduate Student, Dept. of Civil Engineering, Aalborg University, Denmark.
[2]Professor, Dept. of Civil Engineering, Aalborg University, Denmark.
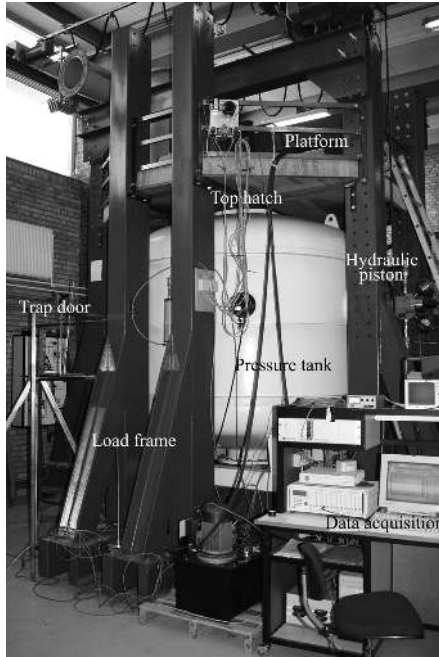[3]PhD Fellow, Dept. of Civil Engineering, Aalborg University, Denmark.

Figure 1: The pressure tank installed in the Geotechnical Engineering Laboratory at Aalborg University, Denmark.
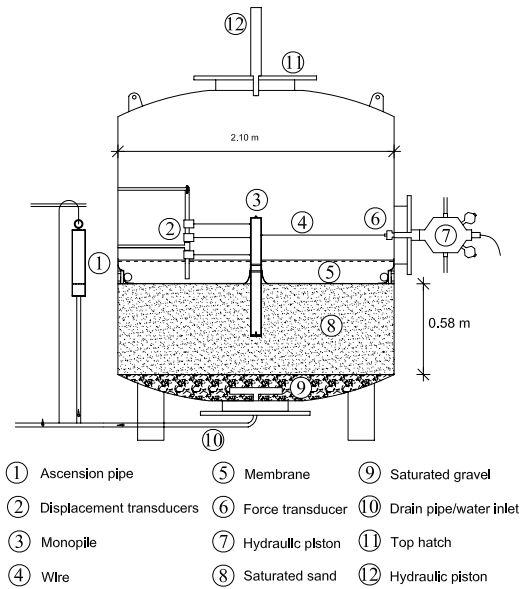

①	Ascension pipe	⑤	Membrane	⑨	Saturated gravel
②	Displacement transducers	⑥	Force transducer	⑩	Drain pipe/water inlet
③	Monopile	⑦	Hydraulic piston	⑪	Top hatch
④	Wire	⑧	Saturated sand	⑫	Hydraulic piston

Figure 2: Cross sectional view of the pressure tank and the test setup.

2 Test Programme

Scale effects occur when conducting small-scale tests in sand at 1 g. At low stress levels the soil parameters, in particular the internal angle of friction, will vary strongly with the effective stresses. Therefore, it is an advantage to increase the effective stresses to a level where the internal angle of friction is independent of the stress variations. This increase in stresses will minimise the fluctuations of the measurements as well. To make the increase in stress level possible the tests are conducted in a pressure tank, cf. Fig. 1.

The tests are carried out at stress levels of 0 kPa, 50 kPa, and 100 kPa, and the results are presented in this paper. The tests are quasi-static tests on two closed-ended aluminium pipe piles with outer diameters of 40 mm and 100 mm and a slenderness ratio of 5, corresponding to embedded lengths of 200 mm and 500 mm, respectively. The wall thickness of the piles is 5 mm.

The test programme, cf. Tab. 1, is designed to investigate the soil resistance dependency of the pile diameter at different stress levels. The pile diameters in the test programme are chosen to supplement the tests described in Sørensen et al. (2009) where piles with diameters of 60 mm and 80 mm were tested. To some extent the results from these tests are included in this paper.

Table 1: The test programme.

	D [mm]	L/D [-]	P_0 [kPa]
Test 1	100	5	0
Test 2	100	5	50
Test 3	100	5	100
Test 4	40	5	0
Test 5	40	5	50
Test 6	40	5	100

Figure 3: The 40 mm pile installed in the sand in the pressure tank.
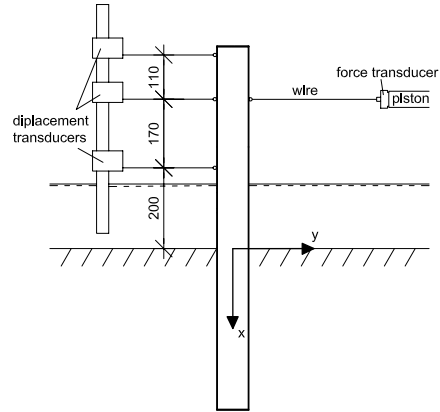

Figure 4: Setup for measuring the lateral deflection of the pile at three levels. The measurements are given in mm.

3   Tests in Pressure Tank

The tests are carried out in a pressure tank installed in the Geotechnical Engineering Laboratory at Aalborg University, Denmark, cf. Fig. 1. The tank has a height of 2.5 m and a diameter of 2.1 m. The tank is placed in a load-frame on a reinforced foundation separated from the rest of the floor in the laboratory.

3.1   Test Setup

Inside the tank a 0.58 m thick layer of fully saturated sand with a layer of highly permeable gravel underneath was located. A cross sectional view of the pressure tank and test setup can be seen in Fig. 2.

The test piles were installed in the sand layer, cf. Fig. 3. A lateral load was applied by means of a wire connected in series to a hydraulic piston through a force transducer. The deflection of the piles was measured by displacement transducers attached in three different levels above soil surface, cf. Fig. 4 and Fig. 5. Thereby, three load-deflection relationships were obtained. To make the soil preparation and pile installation possible the platform mounted on top of the pressure tank, cf. Fig. 1, was used.
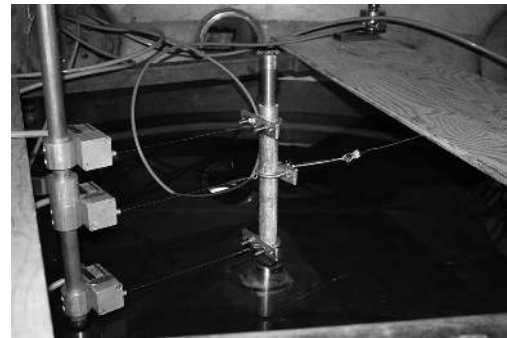

Figure 5: The 40 mm pile instrumented with three displacement transducers.

3.2   Increase   of   the   Effective   Stresses

The increase of the effective stresses in the soil was obtained by placing an elastic, rubber membrane on the soil surface. The membrane was sealed around the pile and against the side of the tank causing the fully saturated soil to be sealed from the air in the upper part of the tank, cf. Fig. 6. Water was poured in on top of the membrane to ensure fully saturated sand even if there were small gabs in the membrane or in the sealing between membrane and tank. Moreover, the dynamic viscosity of water is approximately 55 times greater than of air, and thereby the water minimised the flow through gabs.

Figure 6: The membrane placed on the soil surface and sealed around the pile by hose clips and sealed against the side of the tank by a fire hose.

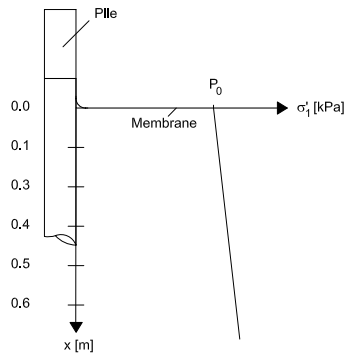**Figure 7:** The openings in the tank hermetically sealed.

Figure 8: Variation of effective vertical stresses.

Figure 9: The ascension pipe connected to the tank to maintain hydrostatic pore pressure in the soil during the tests.

The effective stresses were then increased by closing the openings in the tank, as shown in Fig. 7, and applying an air pressure of 50 kPa and 100 kPa, respectively. Because the pressure in the upper part of the tank made the membrane resemble an applied surface load, a homogeneous increase of the effective stresses was obtained.

3.3 Hydrostatic Pore Pressure

To maintain a hydrostatic pore pressure in the soil, an ascension pipe was connected to the tank and, thereby, the water flowing through the gabs was led out of the tank. This way the soil remained fully saturated and the stresses were applied as effective stresses only. The variation of the effective vertical stresses in the soil layer is shown in Fig. 8, where P_0 denotes the applied overburden pressure. The ascension pipe can be seen in Fig. 9.

4   Measuring System

The hydraulic piston used to actuate the pile was controlled by a predefined displacement and it acted at a vertical eccentricity of 370 mm above the soil surface, cf. Fig. 4. The force transducer connecting the wire and the hydraulic system in series, cf. Fig. 2 ⑥, was a HBM U2B 10 kN for tests on the 40 mm pile and a HBM U2B 20 kN for the 100 mm pile.
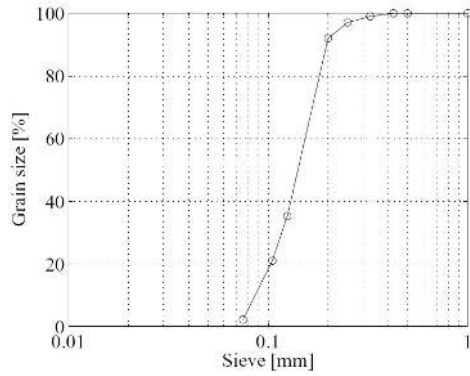
Figure 10: Distribution of Baskarp Sand No. 15 found by sieve analysis. (Ibsen and Bødker, 1994)

Figure 11: The pile fixed by the hydraulic piston.

The displacement transducers, cf. Fig. 2 ②, were of the type WS10-1000-R1K-L10 from ASM GmbH. For measuring the pressure in the tank a HBM P6A 10 bar absolute pressure transducer was employed in the first test, and a HBM P3MBA 5 bar absolute pressure transducer was employed in the remaining tests reducing the fluctuations of the measurements. The sampling frequency was 10 Hz.

5 Soil conditions

The sand used in the tank was Baskarp Sand No. 15. The material properties for Baskarp Sand No. 15 are well-defined from previous tests in the laboratory at Aalborg University. A representative distribution of the grains found by sieve analysis is shown in Fig. 10. The uniform grading of the grains makes it possible to obtain a homogeneous compaction of the soil. The hydraulic conductivity is $k \approx 6 \cdot 10^{-5}$ m/s. The loading velocity was $1 \cdot 10^{-5}$ m/s, thus, the soil was considered drained during the tests. The material properties are given in Tab. 2.

Table 2: Material properties for Baskarp Sand No. 15. (Andersen et al., 1998)

Specific grain density d_s [-]	2.64
Maximum void ratio e_{max} [-]	0.858
Minimum void ratio e_{min} [-]	0.549
$d_{50} = 50\%$-quantile [mm]	0.14
$U = d_{60}/d_{10}$ [-]	1.78

5.1 Soil preparation

Prior to each test the soil was loosened by an upward gradient of 0.9. Hereafter, it was vibrated mechanically to ensure fully saturated soil and a homogeneous compaction.

The pile was installed in the centre of the tank. During installation, a gradient of 0.9 was applied to minimise the pressure on the closed end of the pile. Hereby, the toe resistance and the skin friction along the pile were minimised. After installation the soil was vibrated mechanically, cf. Fig. 12, to minimise disturbances in the soil emerged from the pile installation. While vibrating the pile was secured in its upright position by means of the hydraulic piston mounted through the top hatch of the tank, cf. Fig. 2 ① and Fig. 11.

To control the homogeneity and the compaction of the soil, cone penetration tests (CPT) were conducted. The setup of the CPT-device can be seen in Fig. 13. A total
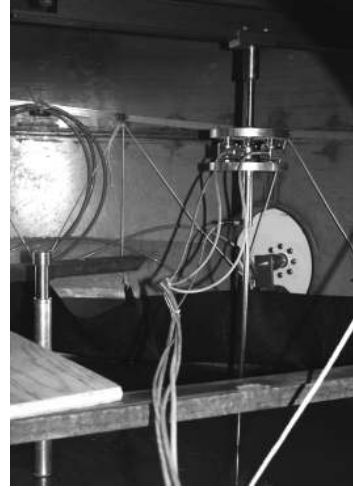
Figure 12: Vibration of the soil.

Figure 13: The setup of the CPT-device in the pressure tank.

of six CPT's were conducted prior to each test. Four were conducted in a distance of 500 mm from the centre of the pile, cf. Fig. 14. The remaining two CPT's were conducted 160 mm and 200 mm from the pile centre for the 40 mm and the 100 mm pile, respectively. Both were conducted on the neutral side of the pile. The probe diameter of the CPT-devise was 15 mm.

In Fig. 15 the cone resistance of the CPT's conducted prior to test 5 shows a homogeneous compaction of the soil. Fig. 16 shows the mean value of the cone resistance, q_c, prior to each of the six tests described in this paper and those obtained prior to the tests described in Sørensen et al. (2009). The figure shows that q_c of the soil was approximately the same for the six tests conducted on the 40 mm pile and the 100 mm pile. Though, compared to the CPT's conducted in Sørensen et al. (2009) they were higher.

In Tab. 3 the soil parameters derived on basis of the CPT's are presented. The parameters are derived in accordance to Ibsen et al. (2009), cf. Eqs. 1 to 5, which are derived empirically for Baskarp Sand No. 15. The formulation for the tangential modulus of elasticity, E_0 cf. Eq. 6, is given by Brinkgreve and Swolfs (2007).
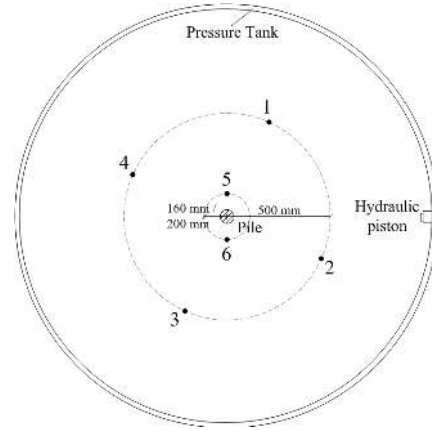

Figure 14: The positions of the six CPT's conducted prior to each test.

$$\varphi_{tr} = 0.152 \cdot I_D + 27.39 \cdot \sigma_3'^{-0.2807} \quad (1)$$
$$+ 23.21$$

$$\psi_{tr} = 0.195 \cdot I_D + 14.86 \cdot \sigma_3'^{-0.09764} \quad (2)$$
$$- 9.946$$

$$I_D = c_2 \left(\frac{\sigma_1'}{(q_c)^{c_1}} \right)^{c_3} \quad (3)$$

$$\gamma' = \frac{d_s - 1}{1 + e_{in\text{-}situ}} \gamma_w \quad (4)$$

$$E_{50} = \left(0.6322 \cdot I_D^{2.507} + 10920 \right) \cdot \quad (5)$$
$$\left(\frac{c \cdot \cos \varphi_{tr} + \sigma_3' \cdot \sin \varphi_{tr}}{c \cdot \cos \varphi_{tr} + \sigma_3'^{\,ref} \cdot \sin \varphi_{tr}} \right)^{0.58}$$
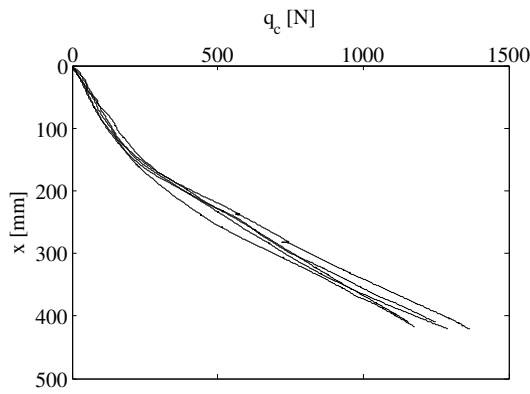
$$E_0 = \frac{2 \cdot E_{50}}{2 - R_f} \quad (6)$$

Figure 15: The cone resistance, q_c, from the CPT's conducted prior to test 5.
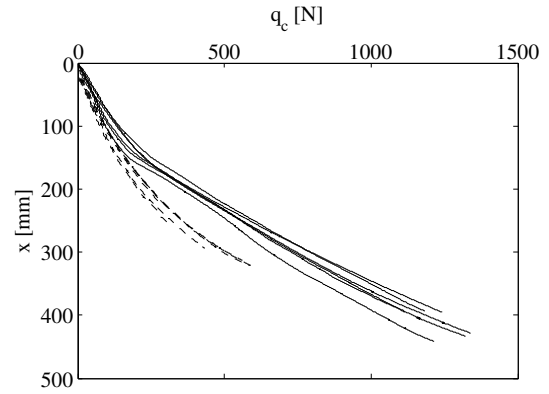

Figure 16: Mean values of the cone resistance, q_c, prior to each test. The solid curves are q_c obtained prior to the tests described in this paper. The dashed curves are q_c obtained prior to the tests described in Sørensen et al. (2009).

φ_{tr} is the internal angle of friction, I_D is the identity index, σ_3' and σ_1' are the effective horizontal and vertical stresses, respectively, and ψ_{tr} is the dilation angle. $(c_1, c_2, c_3) = (0.75, 5.14, -0.42)$, γ' is the effective unit weight of the soil, d_s is the relative density of the soil, $e_{in\text{-}situ}$ is the in-situ void ratio, and γ_w is the unit weight of water. E_{50} is the secant modulus of elasticity, c is the cohesion, and R_f is the failure ratio, which is normally set to 0.9.

By comparing the obtained parameters to the ones derived in Sørensen et al. (2009), given in Tab. 4, it can be seen that the identity indeces, I_D, derived for the present tests are approximately 10 % higher. Because the internal angle of friction, φ_{tr}, and the effective unit weight of the soil, γ', are dependent on I_D these parameters are slightly higher as well. The tangential modulus of elasticity, E_0, is not calculated for the tests without overburden pressure because the low stress level leads to large uncertainties in the determination.

Table 3: Material properties determined from the CPT's conducted prior to the six tests.

D	P_0	φ_{tr}	ψ_{tr}	I_D	γ'	E_0
[mm]	[kPa]	[°]	[°]	[−]	[kN/m^3]	[MPa]
100	0	53.8	19.6	0.86	10.3	-
100	50	50.3	19.0	0.89	10.4	38.2
100	100	47.7	18.3	0.90	10.4	55.6
40	0	54.4	20.4	0.91	10.4	-
40	50	50.4	19.1	0.89	10.4	38.6
40	100	48.0	18.6	0.91	10.4	57.2

Table 4: Material properties determined from the CPT's conducted prior to the six tests conducted in Sørensen et al. (2009).

D	P_0	φ_{tr}	ψ_{tr}	I_D	γ'	E_0
[mm]	[kPa]	[°]	[°]	[-]	[kN/m^3]	[MPa]
60	0	52.6	18.1	0.79	10.2	-
60	50	48.5	16.9	0.79	10.2	25.4
60	100	45.9	16.2	0.79	10.2	41.1
80	0	52.2	17.5	0.76	10.1	-
80	50	48.3	16.7	0.78	10.1	24.9
80	100	45.1	15.3	0.75	10.1	37.4

6 Results

During the tests, prescribed displacements were applied to the pile and, thereby, the soil was brought to failure, then unloaded and reloaded. Hereby, an estimation of the ultimate soil resistance and the elastic behaviour of the soil can be obtained.
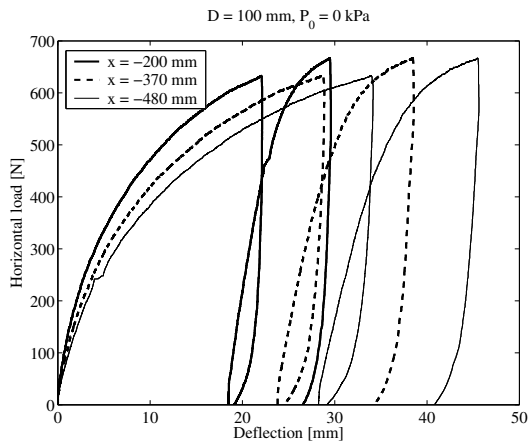
Figure 17: Load-deflection relationships for the 100 mm pile at P_0 = 0 kPa.

Figure 18: Normalised relationships between load (H/H_{max}) and deflection (y/D) measured at the height of the hydraulic piston ($x = -370$ mm) for the 100 mm pile.

In Fig. 17 the load-deflection relationships for test 4 are shown. Firstly, it can be seen that, when unloading and reloading, the load-deflection curves reaches the original curves. Secondly, the upper displacement transducer recorded the largest deflection, while the lower transducer recorded the smallest. This is in agreement with the expected results.

The normalised relationships between load, H/H_{max}, and deflection, y/D, at the level of the hydraulic piston ($x = -370$ mm) for test 1 to 3 are shown in Fig. 18. The test without overburden pressure gives a more curved graph than the tests with overburden pressures. This is caused by the low stress level, at which the dilation of the soil is larger.

6.1 Plastic Response and Pile Capacity

The plastic behaviour of the soil depends on the applied overburden pressure. For the case without overburden pressure the plastic deformation after the first unloading is approximately 85 % of the total deformation after the first loading. For the cases were overburden pressures of 50 kPa
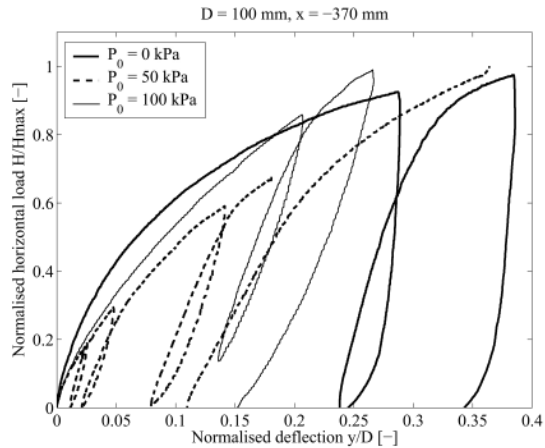
and 100 kPa were applied the plastic deformation is 50 % and 60 %, respectively, of the total deformation after the first loading, cf. Fig. 18.

In Fig. 18 it can be observed that several loading-reloading curves are present for the test at 50 kPa. The reason for this deviation compared to the remaining tests is that the test was run in three stages because of problems with the wire transferring the load to the pile. During the first run the wire was dragged out of its bracket. Therefore, the applied displacement was obtained in the extension of the wire, which resulted in very small deflections of the pile. During the second run the wire deformed, again leading to small deflections of the pile. A last run was conducted and the wanted deflection of the pile was obtained.

Figs. 19 and 20 present the dependency of the overburden pressure on the lateral load. As expected, the capacity of the soil increases with increasing overburden pressure. The difference between the lateral load for the tests without overburden pressure compared to the ones with overburden pressures of 50 kPa and 100 kPa, respectively, is determined for 10 mm de-
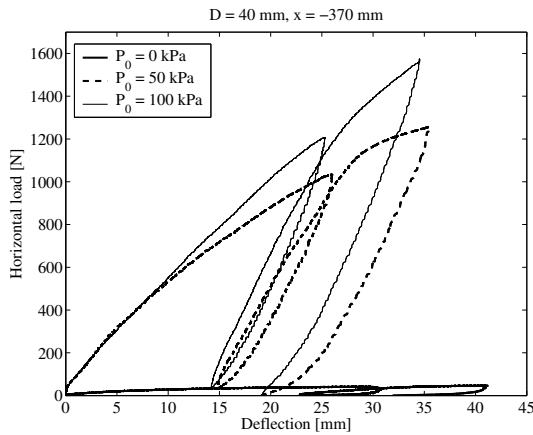
Figure 19: Load-displacement relationships at different overburden pressures measured at the level of the hydraulic piston ($x = -370$ mm) for the 40 mm pile.
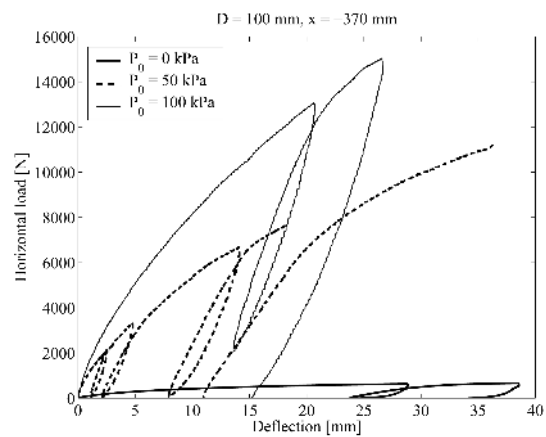

Figure 20: Load-displacement relationships at different overburden pressures measured at the level of the hydraulic piston ($x = -370$ mm) for the 100 mm pile.

flection at the level of the hydraulic piston, i.e. $x = -370$ mm. The lateral load increases with a factor of 17 for the 40 mm pile for 50 kPa and 15 for the 100 mm pile. For 100 kPa the load increases with a factor of 18 and 20 for the 40 mm pile and the 100 mm pile, respectively.

6.2 Uncertainties for the 40 mm Pile

Conducting tests on the 40 mm pile was difficult because little disturbance of the soil would cause large uncertainties for the obtained results due to the small soil volume activated during failure. Fig. 19 shows the load-deflections relationship for the 40 mm pile. The figure shows an unexpected appearance of the graph for the test at 100 kPa as the graph for the first loading describes nearly a straight line. Before this test the pile got stuck in the hydraulic piston and when releasing it the surrounding soil was disturbed. This disturbance might have caused a decrease of the strength in the soil. Thereby, the graph is straight till the point where the pile obtained a deflection large enough to activate the undisturbed soil further away from the pile. Therefore, the results from

test 6 are not considered to represent the correct behaviour of an undisturbed soil.

6.3 Comparison of Test Results

In Fig. 21 the results for the tests without overburden pressure are compared to the results obtained by Sørensen et al. (2009) for 60 mm and 80 mm piles. As expected, the lateral load necessary to obtain a deflection of the pile increases with increasing pile diameter.

Figs. 22, 23, and 24 shows the normalised relationships between the lateral load, H, and the deflection, y, determined at the level of the hydraulic piston for the three stress levels. The normalised formulation for the load, Eq. 7, is chosen because the load is assumed dependent on the soil volume activated during failure, and the stresses in the soil. This assumption provides the expression $LD\sigma'$ that can be rewritten to $LD\gamma'L = L^2D\gamma'$.

$$\text{Normalised load} = \frac{H}{L^2D\gamma'} \qquad (7)$$

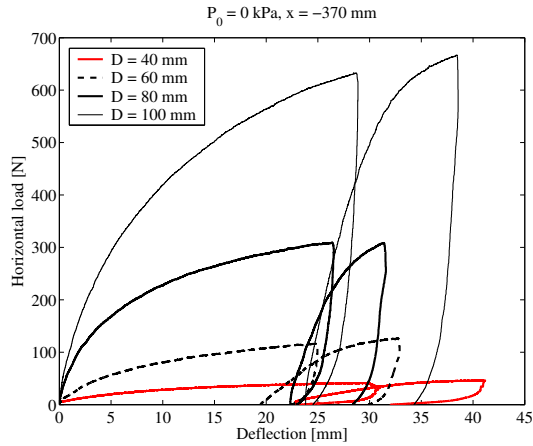$$\text{Normalised deflection} = \frac{y}{D} \qquad (8)$$

9

Figure 21: Load-deflection relationships for the four piles at P_0 = 0 kPa.
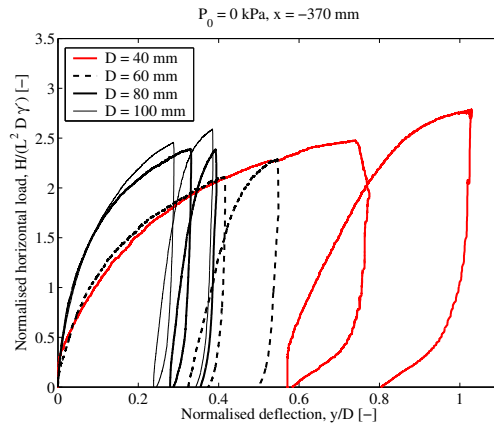

Figure 22: Normalised relationships between load (H/H_{max}) and defection (y/D) measured at the level of the hydraulic piston for the tests at P_0 = 0 kPa.

Figure 23: Normalised relationships between load (H/H_{max}) and deflection (y/D) measured at the level of the hydraulic piston for the tests at P_0 = 50 kPa.
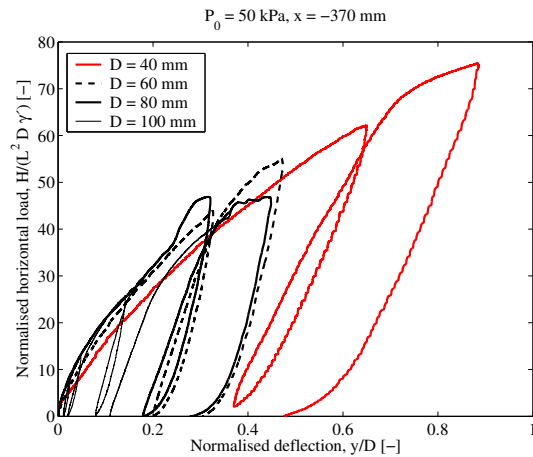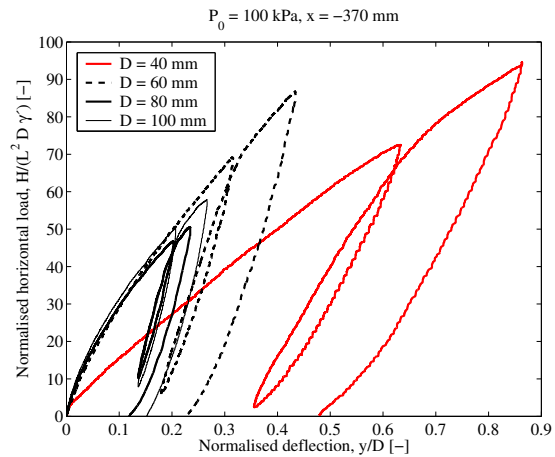

Figure 24: Normalised relationships between load (H/H_{max}) and deflection (y/D) measured at the level of the hydraulic piston for the tests at P_0 = 100 kPa.

Fig. 22 shows deviations between the normalised curves for the four piles without overburden pressure. The curves seems to be grouped in pairs. The 80 mm pile and the 100 mm pile are similar at the initial part of the curves, but deviates at larger deflections. The curves for the 40 mm and the 60 mm pile are similar, but this might be caused by the fact that the identity index for the soil was approximately 10 % larger for the test on the 40 mm pile than for the test on the 60 mm pile, cf. Tabs. 3 and 4.

The reason for the deviations could be the diffenrece in the soil volume activated during failure and the different embedded lengths for the four piles, which causes deviations of the reached stress levels.

In Fig. 23 it can be seen that when applying an overburden pressure of 50 kPa the initial part of the graphs are almost similar. The smaller deviations indicate that the accuracy of the results increases when overburden pressure is applied. For the tests with overburden pressure of 100 kPa the curves are coinciding for the tests on

10

the 60 mm, 80 mm, and 100 mm piles. This implies that the accuracy of the test results increases with increasing overburden pressure. The deviation of the curve for the 40 mm pile is caused by the disturbance of the soil before the test.

In spite of the inaccurate results for the tests without overburden pressure and for the tests of the 40 mm pile, the normalised relationships indicate that the lateral load is proportional to the embedded length squared and the pile diameter, cf. Eq. 7. Furthermore, they indicate that the accuracy of small-scale testing increases with increasing overburden pressure. In future research it is therefore recommended to conduct similar tests with higher overburden pressure applied.

7   Conclusion

The paper presents results from six small-scale quasi-static tests on laterally loaded piles in sand. The aluminium piles had outer diameters of 40 mm and 100 mm, respectively, and a slenderness ratio, L/D, of 5. The tests were conducted in a pressure tank with effective stress levels of 0 kPa, 50 kPa, and 100 kPa.

By increasing the effective stresses in the soil the problems with the non-linear yield surface for small stress levels were avoided. The increase of the effective stress levels were succesfully obtained by separating the sand from the upper part of the tank by an elastic membrane.

The problems with the non-linear yield surface were seen in the results for the tests without overburden pressure, as the curves for the normalised relationships were not similar. The similarity for the normalised results were obtained for the tests with overburden pressure of 100 kPa, and it can be concluded that accuracy in small-scale testing increases with increasing overburden pressure. Therefore, in future research

it is recommended to conduct small-scale tests with higher overburden pressure applied.

The uncertainties when conducting tests on the 40 mm pile were high, because small disturbances of the soil led to results in disagreement to the other test results. Thereby, it is difficult to draw reasonable conclusions from these tests. In further research small-scale tests should be conducted on piles with larger diameters.

Both the test results obtained for the 100 mm pile and the test results obtained by Sørensen et al. (2009) indicates that the lateral load acting on the pile is proportional to the embedded length squared times the pile diameter.

8   Acknowlegdements

Bibliography

Andersen, A., Madsen, E. and Schaarup-Jensen (1998), 'Eastern Scheldt Sand, Baskarp Sand No. 15', *Data Report 9701 Part 1* . Geotechnical Engineering Group, Aalborg University.

API (1993), *Recommended Practice for Planning, Designing and Constructing Fixed Offshore Platforms – Working Stress Design*, American Petroleum Institute.

Brødbæk, K., Møller, M., Sørensen, S. and Augustesen, A. (2009), 'Evaluation of p-y relationship in cohesionless soil', *DCE Technical Report No. 57* . Aalborg University.

Brinkgreve, R. B. J. and Swolfs, W., eds (2007), *PLAXIS 3D FOUNDATION, Material Models manual, Version 2*, PLAXIS b.v.

DNV (1992), *Foundations*, Det Norske Veritas. Classification Notes No. 30.4.

Ibsen, L. B., Hanson, M., Hjort, T. and Thaarup, M. (2009), 'MC-Parameter Calibration for Baskarp Sand No. 15', *DCE Technical Report No.62* . Department of Civil Engineering, Aalborg University.

Ibsen, L. and Bødker, L. (1994), 'Baskarp Sand No. 15', *Data Report 9301* . Geotechnical Engineering Group, Aalborg University.

Sørensen, S., Brødbæk, K., Møller, M., Augustesen, A. and Ibsen, L. (2009), 'Evaluation of the Load-Displacement Relationships for Large-Diameter Piles in Sand', *Civil-Comp Press* . Paper 244.

Recent publications in the DCE Technical Report Series

Brødbæk, K. T., Møller, M., Sørensen, S. P. H. and Augustesen, A. H. (2009) *Review of p-y relationships in cohesionless soil*, DCE Technical Report No. 57, Aalborg University. Department of Civil Engineering

Sørensen, S. P. H., Møller, M., Brødbæk, K. T., Augustesen, A. H. and Ibsen, L. B. (2009) *Evaluation of Load-Displacement Relationships for Non-Slender Monopiles in Sand*, DCE Technical Report No. 79, Aalborg University. Department of Civil Engineering

Sørensen, S. P. H., Møller, M., Brødbæk, K. T., Augustesen, A. H. and Ibsen, L. B. (2009) *Numerical Evaluation of Load-Displacement Relationships for Non-Slender Monopiles in Sand*, DCE Technical Report No. 80, Aalborg University. Department of Civil Engineering